Basic Res Cardiol 96: 405 – 414 (2001)

ORIGINAL CONTRIBUTION

Helena Hänninen
Panu Takala
Markku Mäkijärvi
Juha Montonen
Petri Korhonen
Lasse Oikarinen
Kim Simelius
Jukka Nenonen
Toivo Katila
Lauri Toivonen

Recording locations in multichannel magnetocardiography and body surface potential mapping sensitive for regional exercise-induced myocardial ischemia

Received: 9 October 2000
Returned for revision: 23 October 2000
Revision received: 2 January 2001
Accepted: 19 January 2001

H. Hänninen, MD (✉) · M. Mäkijärvi
P. Korhonen · L. Oikarinen · L. Toivonen
Helsinki University Central Hospital
Division of Cardiology
Cardiovascular Laboratory
P.O. Box 340
FIN 00029 HUS, Finland
E-mail: hahannin@sci.fi

H. Hänninen · P. Takala · M. Mäkijärvi
J. Montonen · P. Korhonen · L. Oikarinen
K. Simelius · J. Nenonen · T. Katila
L. Toivonen
BioMag Laboratory
Helsinki University Central Hospital

P. Takala · J. Montonen · K. Simelius
J. Nenonen · T. Katila
Laboratory of Biomedical Engineering
Helsinki University of Technology

Abstract *Introduction* This study aimed to identify the optimal locations in multichannel magnetocardiography (MCG) and body surface potential mapping (BSPM) to detect exercise-induced myocardial ischemia. *Methods* We studied 17 healthy controls and 24 coronary artery disease (CAD) patients with stenosis in one of the main coronary artery branches: left anterior descending (LAD) in 11 patients, right (RCA) in 7 patients, and left circumflex (LCX) in 6 patients. MCG and BSPM signals were recorded during a supine bicycle stress test. The capability of a recording location to separate the groups was quantified by subtracting the mean signal amplitude of the normal group from that of the patient group during the ST segment and at the T-wave apex, and dividing the resulting amplitude difference by the corresponding standard deviation within all subjects. *Results* In MCG the optimal location for ST depression was at the right inferior grid for the RCA, at the mid-inferior grid for the LCX, and in the middle of these locations for the LAD subgroup (mean ST amplitudes: CAD –80 ± 360fT, controls 610 ± 660fT; $p < 0.001$). In BSPM it was on the left upper anterior thorax for the LAD, left lower anterior thorax for the RCA, and on the lower back for the LCX subgroup (mean ST amplitudes: CAD –39 ± 61 μV and controls 38 ± 38 μV; $p < 0.001$). In MCG the optimal site for T-wave amplitude decrease was the same as the one for the ST depression. In BSPM it was on the middle front for the LAD, on the back for the LCX and on the left abdominal area for the RCA group. In accordance with electromagnetic theory, the largest ST segment and T-wave amplitude changes took place in MCG in locations orthogonal to those in BSPM. *Conclusion* This study identified magnetocardiographic and BSPM recording locations which are sensitive for detecting transient myocardial ischemia by evaluation of the ST segment as well as the T-wave. These locations strongly depend on ischemic regions and are outside the conventional 12-lead ECG recording sites.

Key words Magnetocardiography – body surface potential mapping – coronary artery disease – myocardial ischemia, exercise testing – discriminant index

Introduction

Recent development in the treatment of coronary artery disease (CAD) has increased the importance of noninvasive detection, localization and quantification of myocardial ischemia. In addition to exercise ECG several other methods, including the radionuclide techniques, magnetic resonance imaging, and stress echocardiography, are in daily practice in ischemia detection. All these methods, however, have disadvantages and the development of new techniques to evaluate the extent and location of the ischemic myocardial area more accurately is still warranted.

Magnetocardiography (MCG) is a novel, noninvasive, multichannel mapping technique to record cardiac electromagnetic signals, generated by the same bioelectric currents as the ECG (22). MCG has morphological features similar to ECG, but there are some fundamental differences. MCG is most sensitive to currents which are tangential to the chest. In addition, MCG can detect circular vortex currents, which give no ECG signal (22). Therefore, MCG may show ischemia-induced deviations from the normal direction of depolarization and repolarization better, or in a different manner than ECG (22). MCG is less affected than ECG by conductivity variations caused by lungs, muscles, and skin (4, 19, 20, 22). Furthermore, problems in the skin-electrode contact often encountered in ECG are nonexistent in a fully non-contact MCG (4, 19 20, 22). A magnetically shielded room markedly improves the signal to noise ratio of the sensitive MCG recordings (18).

Body surface potential mapping (BSPM) covers an extensive area of the thorax, offering a comprehensive spatial scope and resolution, while the six precordial leads in the standard 12-lead ECG cover only a small thoracic area. Therefore, BSPM is more sensitive in the detection of transient ischemia and ischemic myocardial damage (5, 6, 11, 16). The diagnostic failure rate in detection of acute ischemia and infarction based solely on standard 12-lead ECG is as high as 30 % (21). Another study with optimal body surface electrode positions reported high sensitivities for the detection of both acute and old myocardial infarctions (10). Interestingly, all these electrode positions were other than the conventional ones of 12-lead ECG.

Since the best sites for detecting myocardial infarction in BSPM are outside the conventional recording locations, this may also concern the detection of acute transient ischemia. Recently, right precordial leads have improved the sensitivity of ischemia detection in patients with right coronary artery stenosis (15). Finding the most informative recording locations in BSPM may help in obtaining the most accurate information with only a few additional leads in clinical exercise testing.

MCG reveals independent, complementary information compared to body surface ECG in ischemic heart disease (2, 7, 9, 14, 23). Combining BSPM and multichannel MCG in a clinical setting allows a comprehensive study of electromagnetic signals generated by the heart. The purpose of this study was to identify the optimal recording locations for these techniques to detect and localize exercise-induced myocardial ischemia.

Table 1 Clinical characteristics of the study groups

Group	All patients	Subgroups			Controls
	(CAD)	LAD	LCX	RCA	
Number	24	11	6	7	17
Age (years)	57 ± 10	53 ± 7	59 ± 7	57 ± 13	55 ± 7
Male / Female	14/10	6/5	3/3	5/2	12/5
LVEF (%)	64 ± 8	63 ± 6	70 ± 9	60 ± 7	66 ± 7
Stenosis (%)	86 ± 13	82 ± 15	90 ± 13	92 ± 5	–

Number of study subjects or mean ± SD. *CAD* coronary artery disease patients, *LAD* patients with left anterior descending coronary artery stenosis, *LCX* patients with left circumflex coronary artery stenosis, *LVEF* left ventricular ejection fraction, RCA=patients with right coronary artery stenosis

Methods

Patients and controls

The study population (Table 1) consisted of 41 subjects: 24 middle-aged patients with single vessel coronary artery disease and 17 age-matched healthy volunteers. All patients had significant (> 50 % luminal diameter) stenosis in one of the main coronary branches (left anterior descending coronary artery, LAD; left circumflex coronary artery, LCX; or right coronary artery, RCA) in the coronary arteriography. At screening, all patients were required to have anginal pain and ECG-documented evidence of ischemia with ≥ 0.1 mV ST-segment depression in symptom-limited upright bicycle ergometry. The inclusion also required that the patients had not suffered a transmural myocardial infarction, did not show abnormal Q-waves or bundle branch block in the 12-lead ECG, and had no wall motion abnormalities or left ventricular hypertrophy in rest echocardiography.

All patients were clinically stable and under appropriate medication during the study: 21 patients were on β-blockers, 5 patients on calcium antagonists, and 19 patients on long-acting nitrates. No significant differences in weight, height, or estimated body surface area existed between the CAD patients and the controls. The healthy controls had no history of hypertension, smoking, or heart disease in the family, and had normal findings in echocardiography as well as in bicycle ergometry. Before inclusion, all patients and controls gave their informed consent.

Magnetocardiography (MCG)

A 67-channel magnetometer was used (Neuromag Ltd, Helsinki, Finland) for the MCG recordings. Patients and controls underwent the measurements in a magnetically shielded room (Euroshield Ltd, Eura, Finland) of the BioMag Laboratory in a hospital environment (18). The sensors, seven co-axial and 60 planar dc-SQUID (Superconducting Quantum Interference Device) gradiometers, record the magnetic-field component perpendicular to the sensor array surface (B_Z) (Fig. 1) (18). The gradiometers are placed on a slightly curved surface with a diameter of 30 cm (18). During the measurements, the patients were lying on a non-magnetic bed. The cardiomagnetometer sensor array was placed as close to the chest as possible allowing deviation from the frontal plane, and the center was positioned 15 cm below the jugular notch and 5 cm left from the midsternal line (Fig. 1). All recordings were band-pass filtered to 0.03-300 Hz and digitized with a sampling frequency of 1000 Hz.

Body surface potential mapping (BSPM)

In the BSPM measurements, unipolar potentials were recorded at 120 locations covering the whole thorax (Fig. 1). In addition, three limb leads were recorded with electrodes on the right and left shoulder and on the left hip. A Wilson central terminal was used as the reference for the unipolar leads. The 120 Ag/AgCl electrodes were mounted on 18 strips with an inter-electrode distance of 5 cm. The strips were placed vertically on the subject's thorax and the dimensions of the upper body determined their horizontal spacing (Fig. 1). The highest electrode density was on the left anterior chest. After band-pass filtering from 0.16 Hz to 300 Hz, the signals were digitized with the sampling rate of 1000 Hz.

Exercise testing

The patients underwent two separate exercise tests for MCG and BSPM recordings in random order. First, a baseline measurement of five minutes was made at rest. Then, patients performed a supine bicycle exercise test pedalling a non-magnetic ergometer designed for exercise MCG recordings. During exercise, the workload was increased stepwise, and the blood pressure was measured every two minutes. The cessation criteria were severe fatigue or dyspnoea, severe chest pain, progressive decrease or abnormal elevation of systolic blood pressure, or repetitive ventricular arrhythmias. Both MCG and BSPM were continuously recorded during the exercise and up to ten minutes in the recovery phase. The rate pressure products in the stress testing were calculated as the product of the systolic blood pressure (mmHg) and heart rate (beats/min) divided by 100.

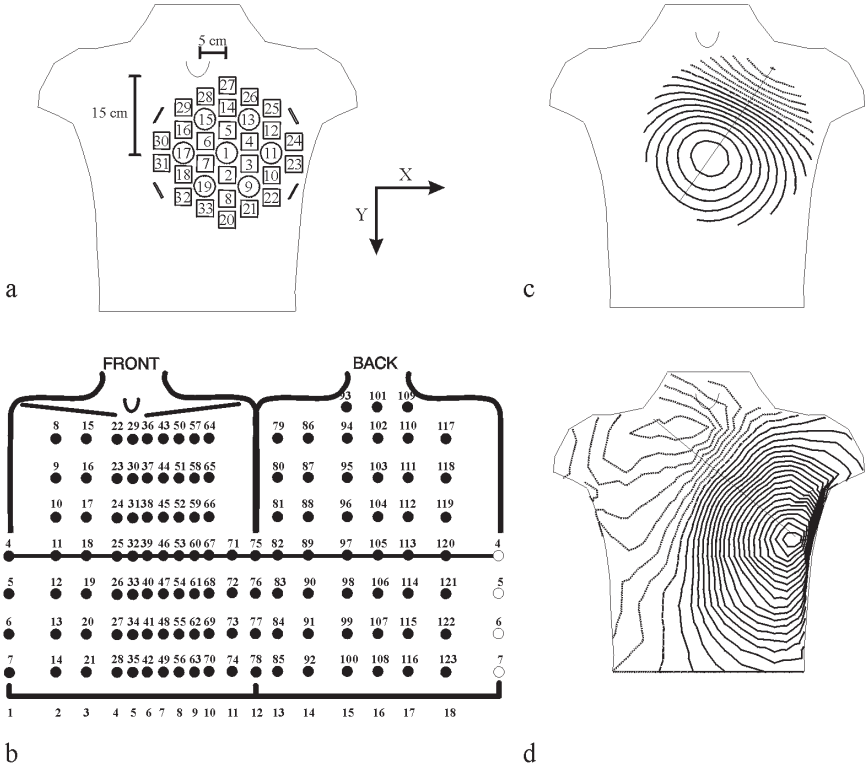

Fig. 1 **a** The sensor arrangement in the cardiomagnetometer. The XY plane is parallel to the sensor surface, while the Z coordinate points into the chest. The circles refer to the seven co-axial gradiometers, while each rectangle denotes two orthogonal planar gradiometers. Numbers refer to measurement locations. **b** The BSPM electrode layout. The 120 electrodes are mounted on 18 strips, which are placed vertically on the subject's thorax. The dimensions of the upper body determine their horizontal spacing. **c** The distribution of the normal component (B_z) of the magnetic field and **d** the distribution of the electric potential over the anterior thorax at the peak of the QRS complex. The zero signal lines as well as signal extrema are orthogonal to each other in MCG and BSPM.

The study was performed according to the Declaration of Helsinki, and the local ethics committee approved it.

Data analysis

First, the data were baseline-corrected and signal-averaged. In the averaging process, a line fitted to the PQ- and TP-intervals was subtracted from the raw data of each cardiac cycle to define the baseline level. In case of a high heart rate, with a shortened TP-segment, a line connecting two consecutive PQ-intervals was used as a baseline. At rest and after the cessation of exercise, 40 cycles of raw data were processed, and about 20 raw data beats were included in the average. All leads judged invalid by visual observation were deleted and replaced by data interpolated from other leads (see the Appendix).

Three phases of the exercise test were analyzed: 1) rest, 2) cessation of exercise, and 3) four minutes post-exercise. Two time intervals of the cardiac cycle were determined: 1) the second quarter from the J-point to the T-wave apex, representing the ST segment, and 2) the T-wave apex, defined as the highest amplitude of the T-wave (Fig. 2). In MCG, these time intervals were determined using the signals of the seven co-axial gradiometers. In BSPM the same time intervals were defined from the six precordial leads equivalent to V1–V6 in the 12-lead ECG. Magnetic isofield and electric isopotential maps of the mean ST segment amplitude and the T-wave apex amplitude were formed using the signal-averaged MCG and BSPM, as described in the Appendix.

Analysis of magnetocardiographic recording

The 67-channel measurement setup, containing both axial and planar gradiometers, was converted to 33-channel setup consisting of axial gradiometers only to make signals in different measurement locations comparable with each other. The conversion was performed using an interpolation method described in the Appendix. The ST segment and T-wave amplitudes were measured from each MCG location at the 33 channel setup.

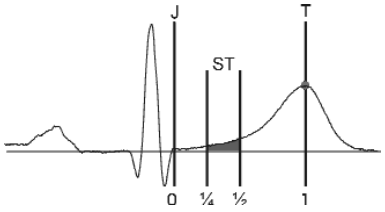

Fig. 2 The analyzed instants of the cardiac cycle were an interval of the ST segment: the second quarter from the J-point to the T-wave apex, and the T-wave apex.

For the evaluation of the typical spatial patterns of the ST segment and the T-wave for healthy controls and each subgroup, the group mean isofield maps were calculated. A discriminant index (DI), suggested by Kornreich et al. (10), indicates the capability of each sensor site to separate a patient subgroup from other patients and controls. The DI was calculated for each subgroup in each recording location. First, the mean amplitude of the control group was subtracted from the mean amplitude of the patient subgroup at each sensor site. The difference was then divided by the standard deviation of signal amplitudes in all subjects. The analysis was performed for both ST segment and T-wave data after stress.

The largest positive discriminant index indicates the optimal location for the ischemia induced ST elevation and T-wave amplitude increase, and the smallest negative discriminant index the optimal location for the ST depression and T-wave amplitude decrease. To illustrate the spatial distribution, discriminant index maps were formed for all CAD patients and for patient subgroups.

Analysis of body surface potential mapping

For the evaluation of the typical isopotential map patterns in patient subgroups and in controls, the group mean electric isopotential maps were calculated in a sim-

Table 2 The ST segment amplitudes at cessation of stress in the optimal MCG channels for ST elevation and depression

	ST amplitude increase					ST amplitude decrease				
Group	DI	Channel	Patients	Controls	p-value	DI	Channel	Patients	Controls	p-value
CAD	0.98	26	−70 ± 470	−700 ± 680	<0.005	−1.14	33	−80 ± 360	610 ± 660	<0.001
LAD	0.95	13	−270 ± 510	−1050 ± 880	<0.01	−1.05	33	−23 ± 330	610 ± 660	<0.005
LCX	0.75	27	−240 ± 420	−710 ± 650	ns	−1.49	8	−350 ± 370	470 ± 520	<0.005
RCA	1.46	26	240 ± 500	−−700 ± 680	<0.01	−1.17	32	−270 ± 480	490 ± 710	<0.01

Channels refer to locations in Fig. 1a. The statistical significance of the amplitude difference comparing patient groups to controls, Mann-Whitney U test. Amplitudes in fT (mean ± SD). *CAD* coronary artery disease patients, *DI* discriminant index, *LAD* patients with left anterior descending coronary artery stenosis, *LCX* patients with left circumflex coronary artery stenosis, *RCA* patients with right coronary artery stenosis.

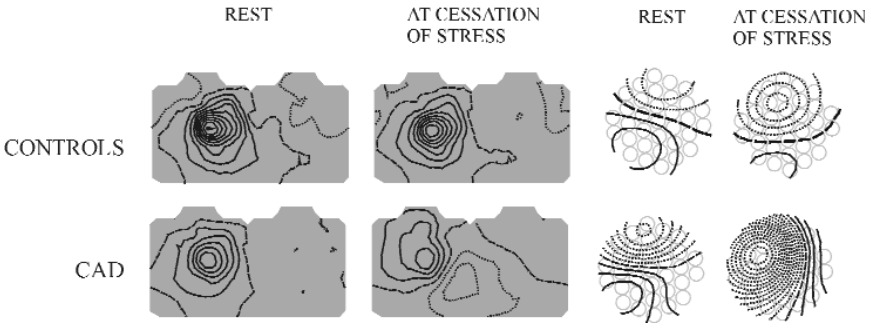

Fig. 3 The group mean isopotential (BSPM) and magnetic isofield (MCG) maps of the ST segment at rest and at cessation of stress. Left: Spatial distribution of the electric potential. Right: Spatial distribution of the magnetic field component B_z. Top: healthy controls; bottom: coronary artery disease patients (CAD). In BSPM, healthy controls have a large positive potential maximum surrounded by zero-potential line at the anterior thorax both at rest and at cessation of stress. In CAD patients the maximum ST depression at cessation of stress is at the left side of the anterior thorax, below precordial standard 12-lead ECG recording locations. In MCG maps, ischemia induced a change in the field orientation and polarity after stress. The step between two isocontour lines is 0.025 μV in BSPM and 0.1 pT in MCG. The positive values are denoted by solid lines and negative values by dotted lines. In MCG, positive values indicate flux towards the chest. Zero potential and zero field line is marked by a dashed line.

ilar manner as the magnetic isofield maps. Discriminant index was also calculated for the electric mapping as described above, and corresponding discriminant maps were formed (10).

Statistical analysis

The Mann-Whitney U test was used for the statistical analysis of parameters. A two tailed p-value < 0.05 was considered statistically significant.

Results

MCG: the ST segment at cessation of stress

The group mean ST segment MCG maps for controls and CAD patients are presented in Fig. 3. The optimal location for ST depression was at the right inferior part of the measurement grid in the RCA group, at the mid-inferior part one sensor site up in the LCX group and in the middle of these locations for the LAD group (Fig. 4, Table 2). The optimal location for ST elevation was found at the left superior part of the measurement grid for the RCA, one sensor site lower for the LAD and in the middle for the LCX group.

MCG: the T-wave four minutes postexercise

The optimal location for T-wave amplitude decrease was at the right inferior part of the grid for the RCA group, at the mid-inferior part one sensor site up in the LCX group and in the middle of these locations for the LAD group (Fig. 5, Table 3). The optimal location for T-wave amplitude increase was at the left superior part of the grid for the LAD group, one sensor site up in the RCA patient subgroup, and at the mid-superior part for the LCX subgroup.

In MCG, the results of the ST segment and T-wave remained accordant to the findings described above also when only the data from the patient subgroup in ques-

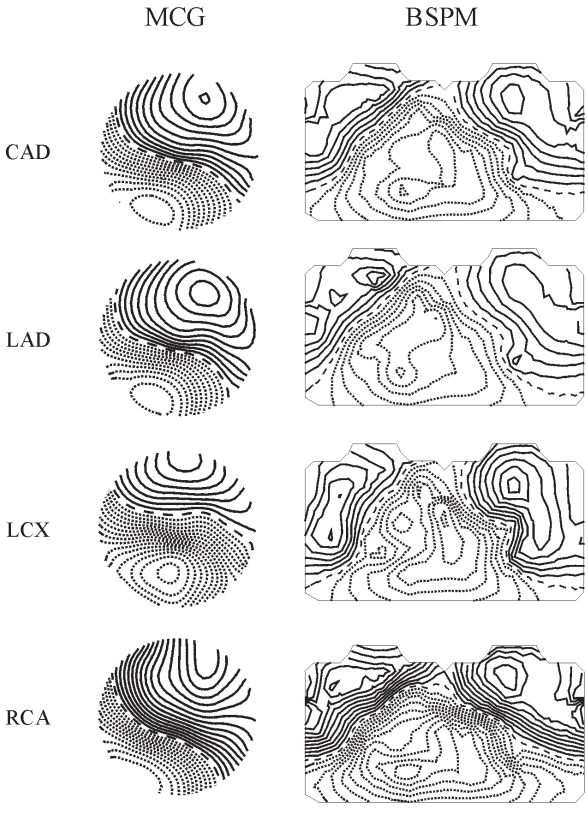

Fig. 4 The discriminant index (DI) maps of the ST segment at cessation of stress. From top to bottom: coronary artery disease patients (CAD), patients with stenosis in the left anterior descending (LAD), left circumflex (LCX), and right (RCA) coronary artery. The channels having the highest or lowest value of discriminant index are the optimal ones to detect changes caused by ischemic injury current. In MCG and in BSPM the best locations for analyzing ST depression were different for each stenosed vessel region, and in BSPM they all were at different sites of the thorax. The step between two isocontour lines is 0.1. Positive values are denoted by solid lines and negative values by dotted lines. Dashed line indicates zero value of DI.

Table 3 The T-wave apex amplitudes 4 minutes postexercise in the optimal MCG channels for T-wave amplitude increase and decrease

	T-wave amplitude					T-wave amplitude				
Group	DI	Channel	Patients	Controls	p-value	DI	Channel	Patients	Controls	p-value
CAD	1.06	25	−1810 ± 1460	−3790 ± 1840	<0.005	−0.92	33	1470 ± 1130	2780 ± 1460	<0.01
LAD	1.15	12	−1010 ± 920	−3160 ± 1990	<0.005	−0.79	33	1660 ± 1100	2780 ± 1460	ns
LCX	0.63	27	−2320 ± 1300	−3400 ± 1860	ns	−1.30	8	560 ± 1970	2400 ± 1140	ns
RCA	1.40	25	−1180 ± 1230	−3790 ± 1840	<0.005	−1.26	32	1060 ± 850	3340 ± 2010	<0.01

Channels refer to locations in Fig. 1a. The statistical significance of the amplitude difference comparing patient groups to controls, Mann-Whitney U test. Amplitudes in fT (mean ± SD). *CAD* coronary artery disease patients, *DI* discriminant index, *LAD* patients with left anterior descending coronary artery stenosis, *LCX* patients with left circumflex coronary artery stenosis, *RCA* patients with right coronary artery stenosis.

tion and the controls were used for calculation of the standard deviation in the DI.

BSPM: the ST segment at cessation of stress

The maximum ST segment depression at cessation of stress was on the average 0.10 ± 0.07 mV in the whole CAD patient group, 0.09 ± 0.07 mV in the LAD group, 0.13 ± 0.09 mV in the RCA group, 0.08 ± 0.03 mV in the LCX group, and 0.05 ± 0.03 mV in the control group.

The group mean ST segment BSPM maps for controls and CAD patients are presented in Fig. 3. The optimal location for ST depression was on the left anterior thorax above the recording locations V4-V5 for the LAD, below V5-V6 for the RCA, and behind V6 for LCX subgroups (Fig. 4, Table 4). The optimal location for ST elevation was in front of the right shoulder for the LAD and RCA subgroups, and on the back for the LCX subgroup.

BSPM: the T-wave four minutes postexercise

The group mean T-wave BSPM maps for the patient subgroups are presented in Fig. 6. The optimal location for T-wave amplitude decrease was on left upper parasternal area for the LAD, on the back for the LCX and on the left abdominal area for the RCA group (Fig. 5, Table 5). The optimal location for T-wave amplitude increase was on the back for the LAD and RCA subgroups, and on the right anterior chest for the LCX group.

The results of the ST segment and T-wave remained accordant to the findings described above also in BSPM when only the data from the patient subgroup in question and the controls were used to calculate the standard deviation for the DI.

Discriminant index map patterns

In MCG, both in the ST segment and at the T-wave apex, the largest amplitude differences between the CAD patients and controls took place over the left shoulder for the ST elevation, and around the lower sternum for the ST depression (Figs. 3 and 4). In BSPM the optimal location for ST elevation was on the right shoulder area up to midsternal line, and for ST depression on the left side of the chest or the back. At the T-wave apex the variation between the optimal locations was more extensive in BSPM than in MCG maps in patient subgroups with different stenosed coronary arteries. The lines connecting

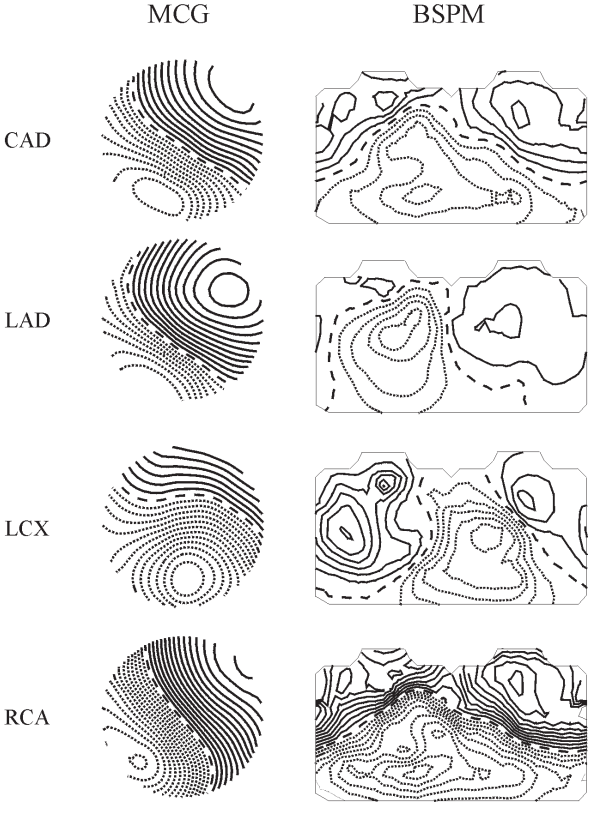

Fig. 5 The discriminant index (DI) maps of the T-wave 4 minutes postexercise, in accordance with Fig. 4. In MCG and in BSPM the best locations for analyzing T-wave amplitude changes were different for each stenosed vessel region, and in BSPM they all were at different sites of the thorax.

Table 4 The ST segment amplitudes at cessation of stress in the optimal BSPM channels for ST elevation and depression

	ST amplitude increase					ST amplitude decrease				
Group	DI	Channel	Patients	Controls	p-value	DI	Channel	Patients	Controls	p-value
CAD	1.26	4	22 ± 39	−41 ± 40	<0.001	−1.19	56	−39 ± 61	38 ± 38	<0.001
LAD	1.15	29	38 ± 32	−30 ± 48	<0.001	−1.15	67	−24 ± 113	88 ± 68	<0.01
LCX	1.35	95	21 ± 33	−16 ± 20	<0.05	−1.24	83	−45 ± 24	−7 ± 27	<0.05
RCA	1.83	8	58 ± 49	−28 ± 37	<0.005	−1.89	74	−90 ± 69	14 ± 35	<0.005

Channels refer to locations in Fig. 1b. The statistical significance of the amplitude difference comparing patient groups to controls, Mann-Whitney U test. Amplitudes in μV (mean ± SD). *CAD* coronary artery disease patients, *DI* discriminant index, *LAD* patients with left anterior descending coronary artery stenosis *LCX* patients with left circumflex coronary artery stenosis, *RCA* patients with right coronary artery stenosis.

Table 5 The T-wave apex amplitudes 4 minutes postexercise in the optimal BSPM channels for T-wave amplitude increase and decrease

	T-wave amplitude					T-wave amplitude				
Group	DI	Channel	Patients	Controls	p-value	DI	Channel	Patients	Controls	p-value
CAD	0.87	104	−20 ± 61	−71 ± 42	<0.05	−0.80	70	33 ± 130	139 ± 110	<0.05
LAD	0.54	104	−39 ± 46	−71 ± 42	ns	−0.96	39	120 ± 205	354 ± 161	<0.01
LCX	1.13	12	39 ± 89	−29 ± 47	ns	−1.09	90	−3 ± 72	67 ± 47	ns
RCA	1.82	104	36 ± 55	−71 ± 42	<0.005	−1.70	70	−86 ± 123	139 ± 110	<0.005

Channels refer to locations in Fig. 1b. The statistical significance of the amplitude difference comparing patient groups to controls, Mann Whitney U test. Amplitudes in μV (mean ± SD). *CAD* coronary artery disease patients, *DI* discriminant index, *LAD* patients with left anterior descending coronary artery stenosis, *LCX* patients with left circumflex coronary artery stenosis, *RCA* patients with right coronary artery stenosis.

largest and smallest DIs in BSPM and in MCG when projected to the chest wall were perpendicular to each other, i.e., the locations were roughly orthogonal in BSPM and in MCG.

The locations with the largest amplitude differences between the patients and controls are not the same as the optimal sites indicated by DIs. Nor are the locations with the largest amplitude differences between rest and different phases of recovery within the patient group the same as the optimal sites indicated by the DI analysis.

The 12-lead ECG recorded simultaneously with MCG

Of the 24 patients, only 7 (29 %) fulfilled the standard ischemia criterion of ≥ 0.1 mV ST-segment depression in the 12-lead ECG during supine stress testing, although all patients had severe angina taking minutes to resolve. The maximum ST segment depressions were, on the average, 0.09 ± 0.08 mV in the whole CAD group and 0.02 ± 0.02 mV in the control group. No significant difference existed between the CAD subgroups. The maximum rate pressure products achieved in supine stress testing for MCG and BSPM were lower than in upright bicycle stress testing (MCG 197 ± 52, BSPM 202 ± 40 and upright ECG 271 ± 54).

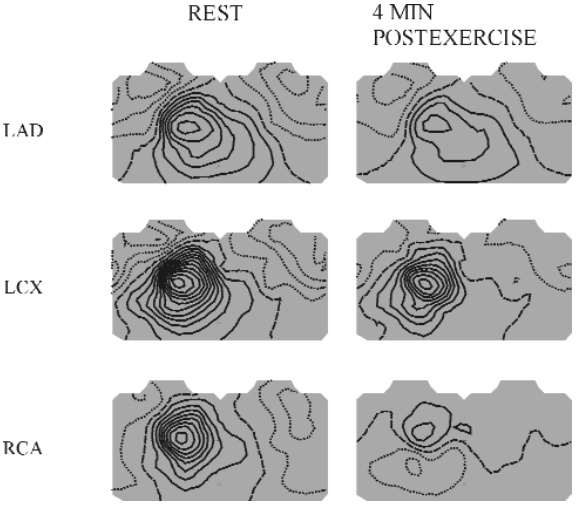

Fig. 6 The group mean electric isopotential maps of the patient subgroups at the T-wave apex. From left to right: Spatial distribution of the electric potential at rest and 4 minutes postexercise. From top to bottom: Patients with stenosis in the left anterior descending (LAD), left circumflex (LCX), and right (RCA) coronary artery. The T-wave changes were most prominent in the RCA subgroup at 4 minutes postexercise. Negative T-waves occurred in the inferior abdominal part of the thorax, and the zero potential line turned from vertical to horizontal after stress. The step between two isocontour lines is 0.025 μV. The positive values are denoted by solid lines and negative values by dotted lines. The zero potential line is marked by a dashed line.

Discussion

This study assessed the optimal recording locations in magnetocardiographic and electrocardiographic mapping to detect transient myocardial ischemia. We analyzed ST segment and T-wave amplitudes in MCG and BSPM in patients with specified ischemic regions and no previous myocardial scar. The discriminant index maps, used to identify most informative recording sites, showed recognizable patterns both in MCG and BSPM. The amplitude changes induced by ischemia separated patient subgroups with stenosis in different coronary arteries from the controls. Both the elevations and depressions of the ST segment as well as changes in T-wave amplitude showed the capability for ischemia detection and localization.

The T-wave had a capability equal to that of the ST segment to separate stenosed vessel regions. In our earlier work the ischemic MCG map rotation increased from the cessation of stress to 2 minutes postexercise and even more to 4 minutes postexercise phase (9). Therefore, we chose to examine T-wave not immediately after stress but at 4 minutes postexercise instead.

ST segment in ischemia detection

In MCG the optimal locations for analyzing both ST depression and elevation in MCG were different in each stenosed vessel region. This confirms a preliminary observation based on the magnetic field rotation (9, 25).

In BSPM the best locations for the analysis of ST depression in each stenosed vessel region were found at different sites on the thorax. This concerned also the analysis of the reciprocal ST elevation. Thus BSPM seems capable of indicating which of the main coronary vessel areas is ischemic. The most informative sites are outside the standard 12-lead ECG. The spatial difference in the BSPM mapping locations was larger than in the MCG, probably due to the larger mapping area.

Contrary to our results, in a BSPM study by Kubota et al. ST segment changes could not localize exercise-induced ischemia in patients with single vessel CAD (13). However, in their study only the location of the maximum ST segment depression was analyzed, and any relative information content, e.g. by discriminant index, was not assessed.

T-wave in ischemia detection

In MCG the optimal locations for detecting the increase or decrease of the T-wave amplitude are different for each stenosed vessel region. The best sites for T-wave amplitude decrease are the same as the ones for the ST depression. The T-wave amplitude increase seems to have slightly greater informative value than the amplitude decrease. Of note is that the T-wave has an equal capability to separate stenosed vessel regions as the ST segment.

In BSPM, the distribution of the optimal locations of the T-wave showed even greater variability between the patient subgroups than those of the ST segment. The maximal T-wave amplitude decrease and increase take place at different sites of the thorax depending on which of the vessel regions is concerned. The sites are not the same as for the ST segment; hence, the T-wave contains information additional to the ST segment.

Variation in isopotential maps during the combined ST-T integral depends on the vessel region (12, 17). Our results indicate that both the ST segment and T-wave contain this information separately. Furthermore, our study extends the localizing capacity, previously demonstrated for old myocardial infarction in BSPM, to transient ischemia.

Complementary nature of magnetic and electric mapping

Several studies have demonstrated that MCG may contain information not detected by BSPM. In a study of Lant et al. (14) the most profound differences between post-infarction patients and controls in BSPM took place during the QRS-complex, while MCG showed larger differences during the repolarization, especially in patients with inferior infarctions. Prolonged ischemic injury, increasing tangential current flow through the spared subendocardial tissue, may have caused these repolarization abnormalities. Brockmeier et al. (1, 2) reported ST segment depressions and T-wave inversions in healthy subjects in MCG mapping after pharmacological stress testing. The authors suggested that the origin of these non-pathogical changes were circular vortex currents, which cannot be seen by ECG. Study by Takala et al. (23) also reported similar amplitude changes in the MCG, not detectable in BSPM after physical exercise.

When injury current is directed from the lower left chest towards the right shoulder it produces ST segment depression in ECG leads V3-V6. In BSPM, covering a larger area of the thorax, the corresponding ST segment elevation is also found in the leads over the upper right thorax. In a homogeneous infinite halfspace such an injury current would induce a magnetic field towards the chest at the upper left part of the thorax, and outwards from the chest at lower right thorax (24). Thus, it would generate a magnetic field map which is orthogonal to the electric potential map. Inhomogeneities such as lungs and blood masses do not affect the magnetic field as much as the electric potential (22). The observation that the extrema of the discriminant index maps in our study were perpendicular in MCG and BSPM supports the

localizing accuracy of electrocardiography despite of the limitations mentioned above.

The optimal MCG sites are mostly at the edge of the MCG sensor. Therefore, even more informative sites for MCG might be found beyond the sensor range, and the relatively small sensor coverage might be disadvantageous for MCG.

Limitations of the study

Localization and quantification of ischemia by isotope ventriculography would have improved the determination of the ischemic myocardial regions. However, the study patients were specifically selected to have a well-defined ischemic area supplied by only one stenotic main coronary branch, and had no significant other abnormalities in coronary anatomy affecting the extent and location of ischemia. The performance of MCG and BSPM in patients with two- or three-vessel coronary artery disease cannot be evaluated on the basis of this study. Supine exercise position may have hampered the ischemia detection partly due to lower rate pressure product. All patients underwent stress-testing twice, in random order, on the same day. Ischemic preconditioning may have had some effect on the latter stress test.

Conclusions

Both electric and magnetic mapping show the ability to detect and localize ischemia. In addition to the region of old myocardial infarction, the location of acute transient myocardial ischemia can also be identified by BSPM and MCG. In BSPM the best recording sites for acute myocardial ischemia are all outside the standard 12-lead ECG. These locations depend on the ischemic regions and may therefore serve to identify the culprit vessels. These sites are not the same for the ST segment and the T-wave; hence the T-wave contains information additional to the ST segment.

Appendix: interpolation with minimum-norm estimation

In this work, the missing or bad leads and virtual 33-channel axial gradiometer signals were interpolated from the measured data using minimum-norm estimation (MNE) (6). MNE is a current density field, J*, defined as a linear combination of the lead fields of the MCG sensors, L_k: $J^*(r) = \Sigma\, \omega_k L_k(r)$. It is the current distribution that has the smallest norm and is compatible with the measured data. We define the next matrix G consisting of inner products between the lead fields of all sensor pairs, L_i and L_j. Then, the weighting coefficients wk are found from the measured signals b^m by $\omega = \Gamma^{-1} b^m$. Since the lead fields in a large array are almost linearly dependent, regularization techniques are needed to produce stable estimates (6).

Interpolation with MNE is based on evaluating the lead fields of virtual sensors, $L_k^{\wedge}$, and composing matrix Γ' from the dot products between measurement and virtual lead fields (3). The interpolated signals are then obtained as $b^e = \Gamma' \Gamma^{-1} b^m$.

For isocontour and axial gradiometer interpolation, the sensor array surface was triangulated. The field component B_z perpendicular to the surface was interpolated at each time instant by assuming a virtual point coil at each node on the triangulated surface.

Acknowledgments The authors thank Ms Rea Katajisto and Ms Leila Sikanen for their assistance in stress testing. This work was supported by the Finnish Cardiac Research Foundation and Aarne Koskelo Foundation.

References

1. Brockmeier K, Comani S, Erne S, Di Luzio S, Pasquarelli A, Romani GL (1994) Magnetocardiography and exercise testing. J Electrocardiol 27: 137–142
2. Brockmeier K, Schmitz L, Chavez J, Burghoff M, Koch H, Zimmermann R, Trahms L (1997) Magnetocardiography and 32-lead potential mapping: repolarization in normal subjects during pharmacologically induced stress. J Cardiovasc Electrophysiol 8: 615–626
3. Burghoff M, Nenonen J, Trahms L, Katila T (2000) Conversion of magnetocardiographic recordings between two different multichannel SQUID devices. IEEE Trans Biomed Eng 47: 869–875
4. Cohen D (1983) Steady fields of the heart. In: Williamson S, Romani G-L, Kaufman L, Modena I (eds) Biomagnetism. An Interdisciplinary Approach Plenum, New York, pp 265–274
5. De Ambroggi L, Bertoni T, Breghi ML, Marconi M, Mosca M (1988) Diagnostic value of body surface potential mapping in old anterior non-Q myocardial infarction. J Electrocardiol 21: 321–9
6. Green LS, Lux RL, Haws CW (1987) Detection and localization of coronary artery disease with body surface mapping in patients with normal electrocardiograms. Circ 76: 1290–1297
7. Haapalahti P, Mäkijärvi M, Korhonen P, Takala P, Montonen J, Salorinne Y, Oikarinen L, Viitasalo M, Toivonen L (2000) Magnetocardiographic QT dispersion during cardiovascular autonomic function tests. Basic Res Cardiol 95 (5): 424–430
8. Hämäläinen MS, Nenonen J (1999) Magnetic source imaging. In: Webster JG (eds) Encyclopedia of Electrical Engineering, Wiley & Sons New York, pp 133–148.
9. Hänninen H, Takala P, Mäkijärvi M, Montonen J, Korhonen P, Oikarinen L, Nenonen J, Katila T, Toivonen L (2000) Detection of exercise induced myocardial ischemia by multichannel magnetocardiography in single vessel coronary artery disease. Annals of Noninvasive Electrocardiology 5 (2): 147–157
10. Kornreich F, Montaque TJ, Rautaharju PM (1991) Identification of first acute Q wave and non-Q wave myocardial infarction by multivariate analysis of body surface potential maps. Circulation 84: 2442–2453
11. Kornreich F, Montaque TJ, Rautaharju PM (1993) Body surface potential mapping of ST segment changes in acute myocardial infarction. Circulation 87: 773–782
12. Kubota I, Hanashima K, Ikeda K, Tsuiki K, Yasui S (1989) Detection of diseased coronary artery by exercise ST-T maps in patients with effort angina pectoris, single-vessel disease, and normal ST-T wave on electrocardiogram at rest. Circulation 80: 120–127
13. Kubota I, Ikeda K, Ohyama T, Yamaki M, Kawashima S, Igarashi A, Tsuiki K, Yasui S (1985) Body surface distributions of ST segment changes after exercise in effort angina pectoris without myocardial infarction. Am Heart J 110: 949–955
14. Lant J, Stroink G, ten Voorde B, Horacek BM, Montague T (1990) Complementary nature of electrocardiographic and magnetocardiographic data in patients with ischemic heart disease. J Electrocardiol 23: 315–322
15. Michaelides AP, Psodamaki ZD, Dilaveris PE, Richter DJ, Andrikopoulos GK, Aggeli KD, Stefanidis CI, Toutouzas PK (1999) Improved detection of coronary artery disease by exercise electrocardiography with the use of right precordial leads. N Engl J Med 340: 340–5
16. Montaque TJ, Johnstone DE, Spencer CA, Miller RM, Mackenzie BR, Gardner MJ, Horacek BM (1988) Body surface potential maps with low-level exercise in isolated left anterior descending coronary artery disease. Am J Cardiol 61: 273–282
17. Nakajima T, Kawakubo K, Toda I, Mashima S, Ohtake T, Iio M, Sugimoto T (1988) ST-T isointegral analysis of exercise stress body surface mapping for identifying ischemic areas in patients with angina pectoris. Am Heart J 115: 1013–1021
18. Nenonen J (1997) Multimodal cardiac source imaging in the BioMag Laboratory. BioMedizinische Technik 42 (Suppl 1): 29–32
19. Nenonen J (1994) Solving the inverse problem in magnetocardiography. IEEE Engineering in Medicine and Biology 13: 487–496
20. Plonsey R (1972) Comparative capabilities of electrocardiography and magnetocardiography. Am J Cardiol 29: 735–736
21. Selker HP (1989) Coronary care unit triage decision aids: how do we know when they work? Am J Med 87: 491
22. Siltanen P (1989) Magnetocardiography. In: MacFarlane P (eds) Comprehensive Electrocardiology Volume II. Pergamon Press New York Oxford Beijing Frankfurt Sao paolo Sydney Tokyo Toronto, pp 1408–1438
23. Takala P, Hänninen H, Montonen J, Mäkijärvi M, Nenonen J, Oikarinen L, Simelius K, Toivonen L, Katila T (1998) Comparison of magnetocardiographic and electrocardiographic exercise mapping in healthy subjects. In: Yoshimoto T, Kotani M, Kuriki S, Karibe H, Nakasato N (eds) Recent Advances in Biomagnetism, Proceedings of the 11th International Congress on Biomagnetism, Tohoku University Press, Sendai, pp 306–309
24. Tripp JH (1983) Physical concepts and mathematical models. In: Williamson S, Romani G-L, Kaufman L, Modena I (eds) Biomagnetism, An Interdisciplinary Approach, Plenum Press, New York, pp 101–139
25. Van Leeuwen P, Hailer B, Lange S, Donker D, Grönemeyer D (1999) Spatial and temporal changes during the QT-interval in the magnetic field of patients with coronary artery disease. Biomedizinische Technik 44: 139–142